articles

molecular pharmaceutics

Evaluation of Cellular Uptake and Gene Transfer Efficiency of Pegylated Poly-L-lysine Compacted DNA: Implications for Cancer Gene Therapy

M. Walsh,*,†,‡ M. Tangney,‡,§ M. J. O'Neill,†,§ J. O. Larkin,‡ D. M. Soden,‡ S. L. McKenna,‡ R. Darcy,|| G. C. O'Sullivan,‡ and C. M. O'Driscoll†

School of Pharmacy, University College Cork, Cork, Ireland, Leslie C. Quick Jnr. Laboratory, Cork Cancer Research Centre, Mercy University Hospital & Bioscience Institute, University College Cork, Cork, Ireland, and Centre for Synthesis and Chemical Biology, Conway Institute, University College Dublin, Dublin, Ireland

Received January 13, 2006

Abstract: Recent success in phase I/II clinical trials (Konstan, M. W.; Davis, P. B.; Wagener, J. S.; Hilliard, K. A.; Stern, R. C.; Milgram, L. J.; Kowalczyk, T. H.; Hyatt, S. L.; Fink, T. L.; Gedeon, C. R.; Oette, S. M.; Payne, J. M.; Muhammad, O.; Ziady, A. G.; Moen, R. C.; Cooper, M. J. *Hum. Gene Ther.* **2004**, *15* (12), 1255−69) has highlighted pegylated poly-L-lysine (C_1K_{30}−PEG) as a nonviral gene delivery agent capable of achieving clinically significant gene transfer levels in vivo. This study investigates the potential of a C_1K_{30}−PEG gene delivery system for cancer gene therapy and evaluates its mode of cellular entry with the purpose of developing an optimally formulated prototype for tumor cell transfection. C_1K_{30}−PEG complexes have a neutral charge and form rod-like and toroid-like nanoparticles. Comparison of the transfection efficiency achieved by C_1K_{30}−PEG with other cationic lipid and polymeric vectors demonstrates that C_1K_{30}−PEG transfects cells more efficiently than unpegylated poly-L-lysine and compares well to commercially available vectors. In vivo gene delivery by C_1K_{30}−PEG nanoparticles to a growing subcutaneous murine tumor was also demonstrated. To determine potential barriers to C_1K_{30}−PEG gene delivery, the entry mechanism and intracellular fate of rhodamine labeled complexes were investigated. Using cellular markers to delineate the pathway taken by the complexes upon cellular entry, only minor colocalization was observed with EEA-1, a marker of early endosomes. No colocalization was observed between the complexes and the transferrin receptor, which is a marker for clathrin-coated pits. In addition, complexes were not observed to enter late endosomes/lysosomes. Cellular entry of the complexes was completely inhibited by the macropinocytosis inhibitor, amiloride, indicating that the complexes enter cells via macropinosomes. Such mechanistic studies are an essential step to support future rational design of pegylated poly-L-lysine vectors to improve the efficiency of gene delivery.

Keywords: Pegylated poly-L-lysine; nanoparticles; endocytosis; macropinocytosis; in vivo transfection

Introduction

Nonviral gene delivery vectors including cationic lipids and polymers are, from a safety perspective, an attractive alternative to viral vectors for cell transfection. However, nonviral vectors remain relatively inefficient at delivering their DNA cargo to the nucleus compared to their viral counterparts. Traditionally poly-L-lysine has been viewed as

* Author to whom correspondence should be addressed. Mailing address: School of Pharmacy, University College Cork, College Road, Cork, Ireland. Tel: +353-21-4904365. Fax: +353-21-4904616. E-mail: melanie.walsh@ucc.ie.

† School of Pharmacy, University College Cork.

‡ Mercy University Hospital & Bioscience Institute, University College Cork.

§ These authors contributed equally to this manuscript.

|| University College Dublin.

10.1021/mp0600034 CCC: $33.50
Published on Web 09/08/2006

a rather inefficient transfection reagent relative to cationic lipids.[2] However, recent reports using pegylated poly-L-lysine have shown increased complex stability and transfection efficiency.[3] Indeed, clinical success has recently been achieved with C_1K_{30}−PEG complexes for cystic fibrosis gene therapy whereby C_1K_{30}−PEG nanoparticles containing the CFTR gene were demonstrated to achieve in vivo transfection and reconstitution of the transmembrane regulator in CF patients.[1] The success of C_1K_{30}−PEG nanoparticles in phase I/II clinical trials may well lead to a renaissance of poly-L-lysine as a gene delivery agent. The novelty of the C_1K_{30}−PEG complexes lies in the fact that they display a neutral charge and are capable of compacting plasmid DNA into toroid-like and rod-like nanoparticles with the rod-like particles having an average width of 20 nm, potentially allowing the nanoparticles to cross the nuclear membrane pore and to transfect nondividing cells. However, the resultant effect of masking the surface charge of poly-L-lysine through the addition of PEG moieties potentially reduces complex binding to the cell surface. This effect has been observed for PEI/DNA complexes by Mishra and coworkers[4] where pegylation significantly reduced gene expression in vitro as a result of reduced cell surface binding. In contrast to this observation, however, other researchers have reported increased solubility and reduced aggregation of complexes in serum upon pegylation, which improves transfection under more physiological conditions.[10,17] While C_1K_{30}−PEG is rapidly emerging as a powerful nonviral gene delivery agent, it is unclear whether this current formulation leads to maximum payload of plasmid to the cell or whether further optimization is required. Such optimization would include the addition of cell surface receptor targeting moieties to specifically target cell surface receptors, fusogenic peptides to aid endosomal escape, and nuclear localization sequences to direct complexes to the nuclear environment. Previous investigations into the transfection efficiency of pegylated poly-L-lysine vector formulations have demonstrated increased transfection efficiency upon modification with receptor binding ligands and fusogenic (KALA) peptides.[5] However, while these formulations have demonstrated improvement over previous poly-L-lysine vectors, success to date has been limited to in vitro cell culture models. It is likely that C_1K_{30}−PEG's in vivo gene transfer achievement may influence future progression of poly-L-lysine gene delivery vectors. Future modifications of this vector to include fusogenic peptides, nuclear localization signals, and indeed targeting ligands to direct complexes to cell surface receptors should be approached with caution as clinically relevant transfection levels are achievable with the unmodified vector. Nevertheless, most researchers agree that tissue specific targeting of gene delivery systems, via either tissue specific promoters[6,7] or overexpressed cell surface receptors,[8,9] is an essential aspect of future therapeutic regimens. Rational design of future C_1K_{30}−PEG DNA delivery systems therefore requires a detailed knowledge of the uptake mechanisms of the complexes together with a clear understanding of the intracellular barriers to efficient transfection.

The overall aim of this work was to formulate and characterize a C_1K_{30}−PEG based DNA delivery system and to investigate its potential for cancer gene therapy. Initial studies investigated the transfection efficiency of C_1K_{30}−PEG nanoparticles compared to optimally formulated lipid and polymeric transfection reagents. This was extended to determine if C_1K_{30}−PEG nanoparticles containing a compacted luciferase reporter plasmid could transfect a growing subcutaneous murine tumor. Finally, to aid future rational design of a C_1K_{30}−PEG vector for cancer gene therapy, we evaluated the uptake mechanism and intracellular pathway taken by rhodamine labeled C_1K_{30}−PEG/DNA complexes to identify intracellular barriers (if any) to gene expression.

Experimental Section

Pegylated Poly-L-lysine. C_1K_{30}PEG5000 (C_1K_{30}−PEG) was synthesized in the laboratory of R.D. at the Conway

(1) Konstan, M. W.; Davis, P. B.; Wagener, J. S.; Hilliard, K. A.; Stern, R. C.; Milgram, L. J.; Kowalczyk, T. H.; Hyatt, S. L.; Fink, T. L.; Gedeon, C. R.; Oette, S. M.; Payne, J. M.; Muhammad, O.; Ziady, A. G.; Moen, R. C.; Cooper, M. J. *Hum. Gene Ther.* **2004**, *15* (12), 1255−69.

(2) Pouton, C. W.; Lucas, P.; Thomas, B. J.; Uduehi, A. N.; Milroy, D. A.; Moss, S. H. *J. Controlled Release* **1998**, *53* (1−3), 289−99.

(3) Mannisto, M.; Vanderkerken, S.; Toncheva, V.; Elomaa, M.; Ruponen, M.; Schacht, E.; Urtti, A. *J. Controlled Release* **2002**, *83* (1), 169−82.

(4) Mishra, S.; Webster, P.; Davis, M. E. *Eur. J. Cell Biol.* **2004**, *83* (3), 97−111.

(5) Lee, H.; Jeong, J. H.; Park, T. G. *J. Controlled Release* **2002**, *79* (1−3), 283−91.

(6) Godbey, W. T.; Atala, A. *Gene Ther* **2003**, *10* (17), 1519−27.

(7) Greenberger, S.; Shaish, A.; Varda-Bloom, N.; Levanon, K.; Breitbart, E.; Goldberg, I.; Barshack, I.; Hodish, I.; Yaacov, N.; Bangio, L.; Goncharov, T.; Wallach, D.; Harats, D. *J. Clin. Invest.* **2004**, *113* (7), 1017−24.

(8) Lu, Y.; Low, P. S. *Cancer Immunol. Immunother.* **2002**, *51* (3), 153−62.

(9) Hattori, Y.; Maitani, Y. *Curr. Drug Delivery* **2005**, *2* (3), 243−52.

(10) Liu, G.; Li, D.; Pasumarthy, M. K.; Kowalczyk, T. H.; Gedeon, C. R.; Hyatt, S. L.; Payne, J. M.; Miller, T. J.; Brunovskis, P.; Fink, T. L.; Muhammad, O.; Moen, R. C.; Hanson, R. W.; Cooper, M. J. *J. Biol. Chem.* **2003**, *278* (35), 32578−86.

(11) Cryan, S. A.; O'Driscoll, C. M. *Pharm. Res.* **2003**, *20* (4), 569−75.

(12) Ziady, A. G.; Gedeon, C. R.; Miller, T.; Quan, W.; Payne, J. M.; Hyatt, S. L.; Fink, T. L.; Muhammad, O.; Oette, S.; Kowalczyk, T.; Pasumarthy, M. K.; Moen, R. C.; Cooper, M. J.; Davis, P. B. *Mol. Ther.* **2003**, 8 (6), 936−47.

(13) O'Brien, M. G.; Collins, C. G.; Collins, J. K.; Shanahan, F.; O'Sullivan, G. C. *Dis. Esophagus* **2003**, *16* (3), 218−23.

(14) Conner, S. D.; Schmid, S. L. *Nature* **2003**, *422* (6927), 37−44.

(15) Grosse, S.; Aron, Y.; Thevenot, G.; Francois, D.; Monsigny, M.; Fajac, I. *J. Gene Med.* **2005**, *7* (10), 1275−86.

(16) Goncalves, C.; Mennesson, E.; Fuchs, R.; Gorvel, J. P.; Midoux, P.; Pichon, C. *Mol. Ther.* **2004**, *10* (2), 373−85.

(17) Mennesson, E.; Erbacher, P.; Piller, V.; Kieda, C.; Midoux, P.; Pichon, C. *J. Gene Med.* **2005**, *7* (6), 729−38.

Institute for Biomolecular Medicine, University College Dublin, according to the protocol of Liu and co-workers.[10] Briefly, C_1K_{30} was synthesized using solid phase peptide synthesis and its purity was evaluated using HPLC. Trifluoroacetate was the counterion of the polycation. For the synthesis of C_1K_{30}−PEG, the C_1K_{30} peptide was dissolved in oxygen free 0.1 M phosphate buffer, pH 7.2 containing 5 mM EDTA. The methoxy-PEG-maleimide (M_r 5000) was dissolved in oxygen free DMSO and added dropwise over 5−10 min to the C_1K_{30} solution with vigorous stirring under an atmosphere of nitrogen. The solution was stored under nitrogen for 24 h prior to purification using a Sephadex G-25 column equilibrated with 0.1% trifluoroacetate. Fractions were analyzed for peptide at 220 nm, and those fractions containing peptide were pooled and lyophilized. The C_1K_{30}−PEG peptide was analyzed by electrospray mass spectrometry for PEG content.

Plasmid Labeling. pGL3-Luciferase reporter plasmid was obtained from Invitrogen. For intracellular uptake and trafficking studies, the plasmid was labeled with a rhodamine fluorophore using the MirusIT DNA labeling kit (Mirus Bio Corporation).

Antibodies. Mouse monoclonal anti-EEA1 was purchased from BD Transduction Laboratories. Mouse monoclonal anti-transferrin receptor was purchased from Zymed Laboratories. Mouse monoclonal (6C4) anti-lysophosphatidic acid (LBPA) was a kind gift form J. Gruenberg. All antibodies were used at their recommended concentrations for immunofluorescence.

Formulation of Compacted DNA Nanoparticles. Nanoparticles were formulated according to the protocol of Liu et al.[10] with some modifications. Briefly 0.9 mL of DNA at a concentration of 0.2 mg/mL in water was added in 100 μL aliquots to a vortexing solution of 0.1 mL of C_1K_{30}−PEG at a concentration of 10.8 mg/mL (mass ratio: 6) in water at room temperature (RT) over 2 min. The final DNA concentration was 0.18 mg/mL. Complexes were allowed to form at RT for 30 min. The compacted DNA nanoparticles were then added to vivaspin 0.5 mL concentrators (100 000 MW cutoff PES membrane) to remove free C_1K_{30}−PEG (Sartorius). Nanoparticles were then brought to the desired DNA concentration with 0.9% NaCl. The C_1K_{30} complexes were formulated as described above but with a starting concentration of 3 mg/mL C_1K_{30}.

Transmission Electron Microscopy. Compacted DNA nanoparticles (10 μL) were added to the carbon surface of 400 mesh copper electron microscope grids (Agar Scientific) for 2 min. Grids were then inverted over a water droplet on Parafilm for 1 min and stained with uranyl acetate (0.04% in methanol) for 2 min. Grids were then dipped in ethanol and blotted dry. Samples were analyzed using a JEOL 2000 FX transmission electron microscope under 40000× and 100000× magnification.

ζ-Potential. ζ-Potential measurements were performed in triplicate using a Zetasizer nano from Malvern instruments. The ζ-potential of the nanoparticles was measured in deionized water that was sterile filtered through a 0.2 μm filter.

Cell Lines and in Vitro Transfection. The murine SV40 virus transformed cell line, COS-7, was obtained from the ECACC. The JBS cell line was established in our laboratory. JBS is a large T-antigen negative variant of the SV3T3 murine fibrosarcoma cells line. Cells were maintained in Dulbecco's modified Eagle's medium supplemented with 10% fetal bovine serum and 2 mM L-glutamine. Cells were grown in 5% CO_2 at 37 °C. For in vitro transfection, cells were seeded, 24 h prior to transfection, at a density of 4×10^4 cells in a 24-well plate and grown in complete medium overnight. One microgram of DNA which was complexed to either lipofectin (according to manufacturer's instructions) at a mass ratio (MR) of 6, DOTAP at a MR of 5.6, JetPEI at a MR of 2, Lipofectamine 2000 at a MR of 3, C_1K_{30} at a MR of 1.67, or C_1K_{30}−PEG at a MR of 6 was incubated with the cells for 4 h. For each transfection reagent, either the optimum mass ratio was established in earlier experiments[11] or the reagent was used according to the manufacturer's instructions. After 4 h, complexes were removed and fresh medium was added to each well. Cells were then incubated for a further 20 h and assayed for luciferase activity using a luciferase assay kit (Promega) according to manufacturer's instructions. To analyze the intracellular uptake of the plasmid DNA upon delivery by the various gene delivery vectors, 4 μg of labeled plasmid was compacted at the relevant mass ratios for each vector used and incubated with COS-7 cells seeded into 6-well plates for 3 h in serum free medium. Cells were then detached from the plates via trypsin, washed in PBS, and analyzed by flow cytometry. Labeled naked DNA was used as a control.

MTT Cytotoxicity Assay. To analyze the toxicity of chlorpromazine, filipin III, and amiloride, COS-7 cells were seeded at a density of 4×10^4 cells in a 24-well plate and grown in complete medium for 24 h. Inhibitors were added at their specified concentrations and incubated for 1.5 h. Following incubation, the medium containing the inhibitors was replaced with fresh complete medium and MTT (Sigma) at a working concentration of 0.5 mg/mL was added to the cells. Cells were incubated for 4 h at 37 °C, 5% CO_2. Following incubation, the cell culture medium was removed and replaced with DMSO for 5 min at RT. The absorbance of the converted MTT dye was read at 562 nm.

Immunofluorescence Microscopy. COS-7 cells were seeded and grown for 24 h on 11 mm glass coverslips at a density of 3×10^4 cells in a 24-well plate. Cells were washed and incubated in serum free medium, and 1 μg of rhodamine labeled DNA that was compacted with C_1K_{30}−PEG at a mass ratio of 6 was added to the wells. Cells were allowed to internalize the nanoparticles for 30 min, 2 h, and 4 h prior to fixing with 3% paraformaldehyde (PFA). Free aldehyde groups were quenched with 50 mM NH_4Cl, and the cells were then permeabilized with 0.05% saponin. Cells that had internalized rhodamine labeled C_1K_{30}−PEG/DNA vectors for 30 min, 2 h, and 4 h were fixed, permeabilized, and incubated

for 1 h at RT in primary antibody diluted in 5% fetal bovine serum (FBS) in phosphate buffered saline (PBS) containing 0.05% saponin. The secondary antibody used was goat anti-mouse conjugated to Alexa 488 dye (Molecular Probes). Coverslips were mounted in MOWIOL (Calbiochem), and images were recorded using a Biorad MCR1024 confocal microscope.

Inhibitor Studies. COS-7 cells were seeded as described under immunofluorescence microscopy. Cells were incubated in serum free medium and were either untreated or pretreated with chlorpromazine (10 μg/mL) to inhibit clathrin vesicles, filipin III (2μg/mL) to inhibit caveolae, or amiloride (50 μM) to inhibit pinocytosis for 30 min (all from Sigma). Cells were then allowed to internalize rhodamine labeled C_1K_{30}−PEG/DNA nanoparticles in the presence of inhibitor for 1 h. Cells were fixed in 3% PFA and subjected to confocal microscopy.

In Vivo Delivery of C_1K_{30}−PEG/DNA Nanoparticles and Analysis of Reporter Gene Expression. For C_1K_{30}−PEG mediated DNA delivery in vivo, subcutaneous JBS tumors (80 mm^3) were administered a single injection to the center of the tumor with 50 μg of C_1K_{30}−PEG compacted pGL3-Luciferase at a mass ratio of 6 in 100 μL of sterile injectable saline at an injection volume equal to the volume of the tumor. In vivo luciferase activity was analyzed 48 h post-transfection as follows: 80 μL of 30 mg/mL firefly luciferin was injected intratumorally. Mice were anaesthetised by ip administration of 200 μg of xylazine and 2 mg ketamine. Ten minutes post luciferin injection, live anesthetized mice were imaged for 1 min using an intensified CCD camera (IVIS Imaging System, Xenogen).

Results

C_1K_{30}−PEG Complexes Are a Mixture of Toroid-like and Rod-like Nanoparticles. Initial characterization of the complexes to obtain size and structural data were obtained by TEM analysis of C_1K_{30}−PEG compacted DNA at a mass ratio of 6 (optimized for mechanistic studies in COS-7 cells). Images yielded a mixture of rod-like and toroid compacted DNA nanoparticles (Figure 1). The rod-like particles displayed a width of ~20 nm and a length of 100−200 nm. The toroid particles had an overall diameter of 30−60 nm. Similar structural data has also been observed by Ziady and co-workers.[12] The overall ζ-potential of these polyplexes approached zero with an average ζ-potential of -0.756 ± 0.125 mV.

C_1K_{30}−PEG Mediated Transfection Is Highly Efficient. To evaluate the transfection efficiency of the neutrally charged C_1K_{30}−PEG nanoparticles compared to that of well-characterized, commercially available cationic lipid and polymer based transfection reagents, pGL3-Luciferase was compacted with C_1K_{30}−PEG and analyzed for luciferase gene expression in COS-7 cells. Nanoparticles were formulated at an optimum mass ratio (ratio of μg of vector:DNA) of 6, and their transfection efficiency was compared to that of optimally formulated lipofectin, DOTAP, PEI (polyethyleneimine), and poly-L-lysine (C_1K_{30}) complexes. Figure 2A demonstrates that the C_1K_{30}−PEG nanoparticles transfected cells with an efficiency equivalent to that of the cationic lipids, lipofectin and DOTAP, displaying over 40-fold greater reporter activity than transfected naked plasmid. Moreover, C_1K_{30}−PEG nanoparticles demonstrated markedly higher transfection activity than unpegylated poly-L-lysine (C_1K_{30}), supporting a role for pegylation in designing poly-L-lysine vectors (Figure 2B). To further investigate the efficiency of DNA delivery by the C_1K_{30}−PEG nanoparticles, labeled plasmid was compacted with either C_1K_{30}−PEG, C_1K_{30}, or Lipofectamine 2000 vectors and incubated with the cells for 3 h prior to analysis by flow cytometry. C_1K_{30} and Lipofectamine 2000 were chosen for comparison to the C_1K_{30}−PEG vector as these displayed the least and most efficient relative transfection efficiency upon luciferase gene expression analysis. In a similar pattern that was observed using luciferase gene expression as an indicator of transfection efficiency, Lipofectamine 2000 displayed the highest amount of DNA uptake into the COS-7 cells with an efficiency of 40% greater than that of naked DNA. Consistent with the gene expression data, relatively poor efficiency of uptake was observed with the C_1K_{30} vector, which demonstrated 2.57% greater uptake than naked DNA. In contrast, the pegylated nanoparticles demonstrated markedly higher efficiency with 7.85% greater uptake of labeled plasmid than naked DNA, again consistent with the pattern observed for luciferase gene expression.

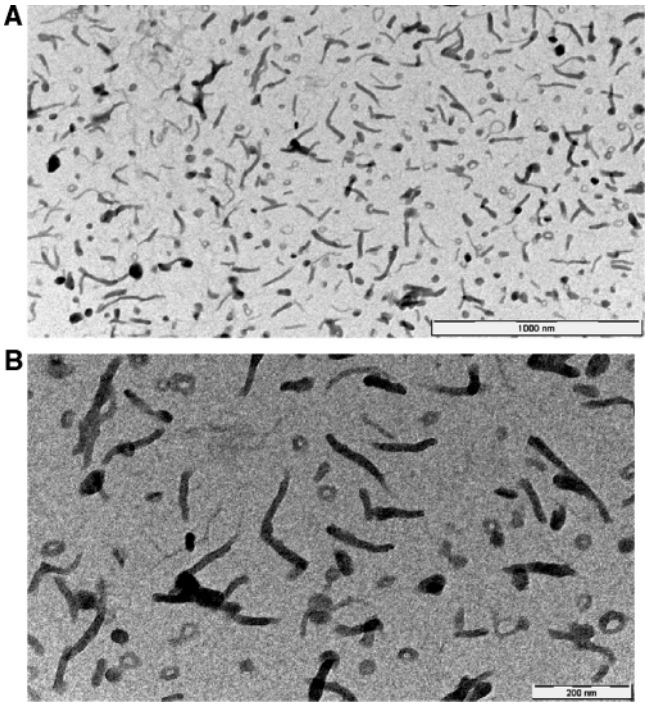

Figure 1. Electron micrograph of the C_1K_{30}−PEG complexes. C_1K_{30}−PEG/DNA complexes at a mass ratio of 6. (A) Magnification of 40 000. The bar represents 1000 nm. (B) Magnification of 100 000. The bar represents 200 nm.

C_1K_{30}−PEG Nanoparticle Transfection of a Growing Tumor in Vivo. To test the ability of C_1K_{30}−PEG to deliver genes to in vivo growing tumors, Balb/C mice were inoculated subcutaneously with JBS fibrosarcoma cells.[13]

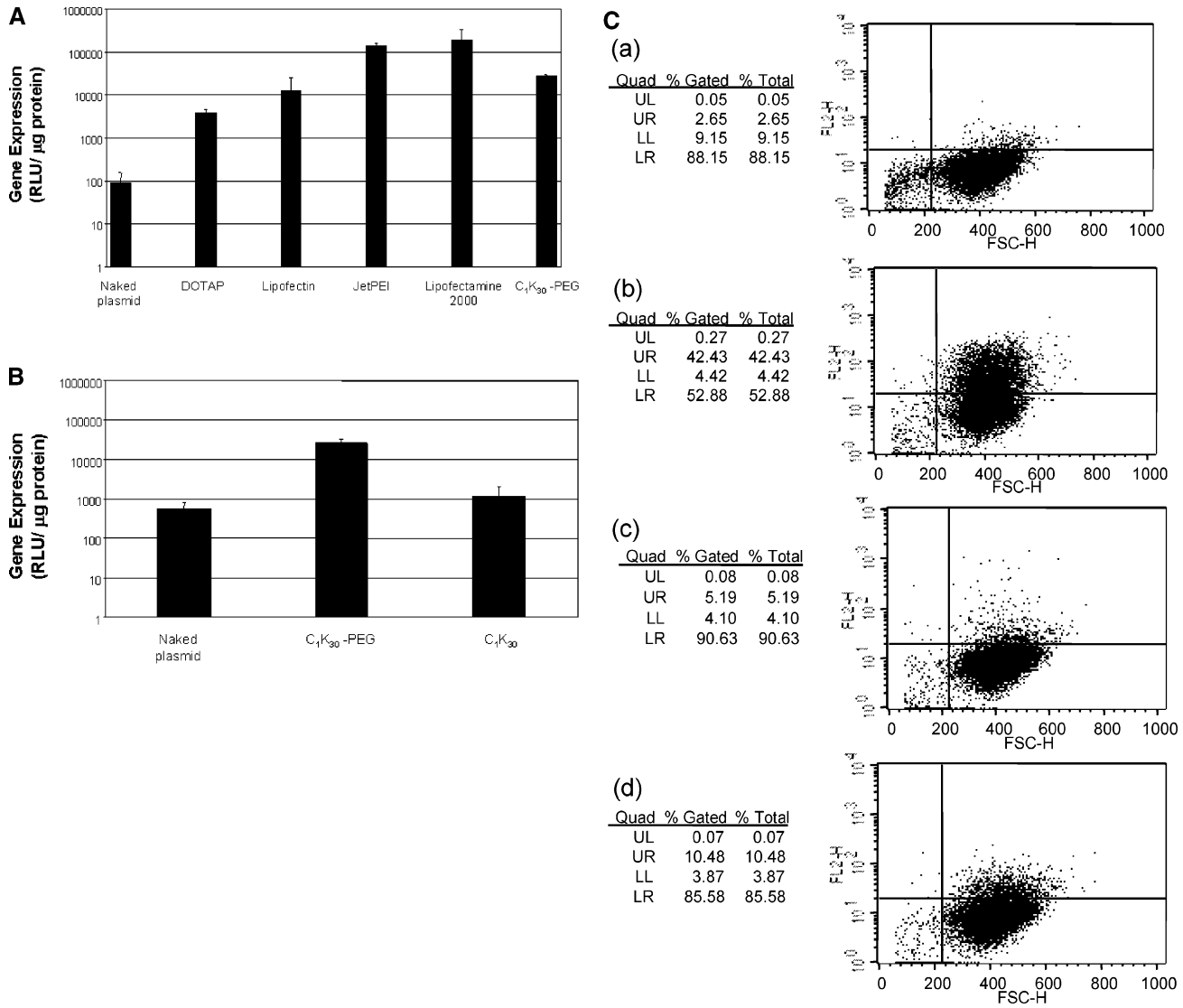

Figure 2. Transfection analysis of C_1K_{30}−PEG compacted DNA nanoparticles. (A) Luciferase gene expression in COS-7 cells following transfection with either lipofectin complexes (mass ratio: 6), DOTAP complexes (mass ratio: 5.6), JetPEI complexes (mass ratio: 2), Lipofectamine 2000 (mass ratio: 3), or C_1K_{30}−PEG compacted pGL3-Luciferase (mass ratio: 6). (B) Luciferase gene expression in COS-7 cells following transfection with naked plasmid, C_1K_{30}−PEG, or unpegylated C_1K_{30} complexes. All transfections were performed in the presence of 10% serum. Luciferase expression was assayed 24 h post-transfection and is expressed as relative light units (RLU) per mg of protein as determined by the BCA assay. Data represent the mean ± SD of triplicate values. Data are representative of at least three independent analyses. (C) Flow cytometric analysis of uptake of labeled plasmid DNA. All complexes were formed as before. (a) Naked labeled DNA, (b) Lipofectamine 2000 compacted DNA, (c) C_1K_{30} compacted DNA, (d) C_1K_{30}−PEG compacted DNA.

Initially, the optimal formulation of the C_1K_{30}−PEG nanoparticles to transfect JBS cells in vitro was determined, and a mass ratio of 6 gave maximum transfection efficiency (not shown). The optimally formulated nanoparticles were then administered to the growing JBS tumor via intratumoral injection. Figure 3 demonstrates in vivo luciferase expression in a representative JBS tumor mass of three mice tested, 48 h following delivery (all three mice were positive). No expression was observed following intratumoral injection of naked DNA.

Intracellular Trafficking of C_1K_{30}−PEG Nanoparticles. Endocytosis is an essential cellular process for the internalization of a number of macromolecules and occurs via two broad categories, phagocytosis (requires specialized cells) or pinocytosis. Pinocytosis itself can be in turn subdivided into categories such as macropinocytosis (molecules > 120 nm), caveolin-mediated endocytosis (molecules ~60 nm), and clathrin-mediated endocytosis (~120 nm).[14] It is generally believed that the latter pathways are more regulated and efficient than macropinocytosis. Indeed, clathrin-mediated endocytic pathways are well-characterized and usually function in receptor-mediated endocytosis of ligands which undergo either recycling to the cell surface or degradation in the lysosomes following trafficking via acidic endosomes.

To delineate the intracellular pathway taken by the C_1K_{30}−PEG nanoparticles following cellular entry, the cellular

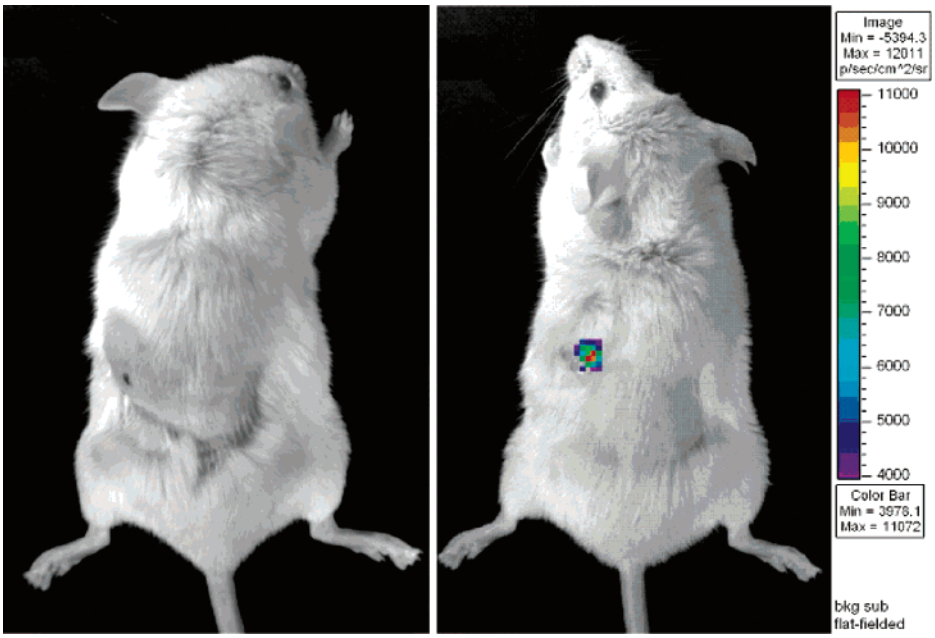

Figure 3. In vivo delivery of a C_1K_{30}−PEG compacted luciferase reporter gene plasmid to murine tumor mass. Nanoparticle transfection in vivo was assessed using whole body imaging of luciferase expression. JBS tumor masses (80 mm^3) were administered a single intratumoral injection of 100 μL containing either 50 μg of naked pGL3-Luciferase (left panel) or 50 μg of C_1K_{30}−PEG compacted pGL3-Luciferase at a mass ratio of 6 (right panel) in sterile injectable saline at an injection volume equal to the volume of the tumor. In vivo luciferase activity was analyzed 48 h post-transfection. Live anesthetized mice were imaged for 1 min using an intensified CCD camera (IVIS Imaging System, Xenogen). Representative mice are shown from groups of three. This image is composed of a pseudocolor image representing intensity of emitted light (red most intense and blue least intense) superimposed on a grayscale reference image.

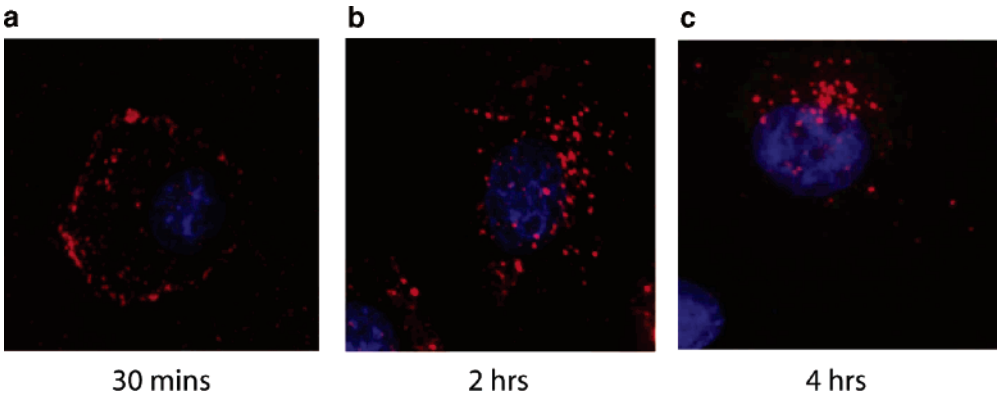

Figure 4. Cellular distribution of rhodamine labeled nanoparticles: COS-7 cells were transfected with rhodamine labeled C_1K_{30}−PEG nanoparticles. At 30 min (a), 2 h (b), and 4 h (c) post-transfection, cells were fixed with PFA, permeabilized, and stained with Hoechst dye to visualize the nucleus.

location of complexed rhodamine labeled DNA at 30 min, 2 h, and 4 h following transfection of COS-7 cells was analyzed (Figure 4). At 30 min post-transfection, a punctate, vesicular rhodamine labeling pattern was observed at the cell's periphery. No significant uptake of nanoparticles into the cell was observed until approximately 2 h post-transfection, at which time the labeling appeared to be more diffuse throughout the cell. At 4 h post-transfection there was a concentration of labeling around the nucleus indicating the intracellular trafficking of the nanoparticles to the perinuclear area. Using the early endosomal marker EEA1, C_1K_{30}−PEG nanoparticles were observed to enter early endosomes 2 h post-transfection, although only partial colocalization of the nanoparticles with early endosomes was observed (Figure 5A). This was not surprising since cellular entry of complexes is a dynamic process. Previous observations have suggested that polylysine polyplexes similar in size to the C_1K_{30}−PEG nanoparticles (100−200 nm) undergo clathrin-mediated endocytosis.[15−17] However, it must be noted that the nature of polyplexes was distinctly different from the C_1K_{30}−PEG vector used in this study, and the polyplexes were themselves either histidylated (maintaining the cationic nature of the vector) or modified with a receptor binding ligand which may itself promote receptor-mediated endocy-

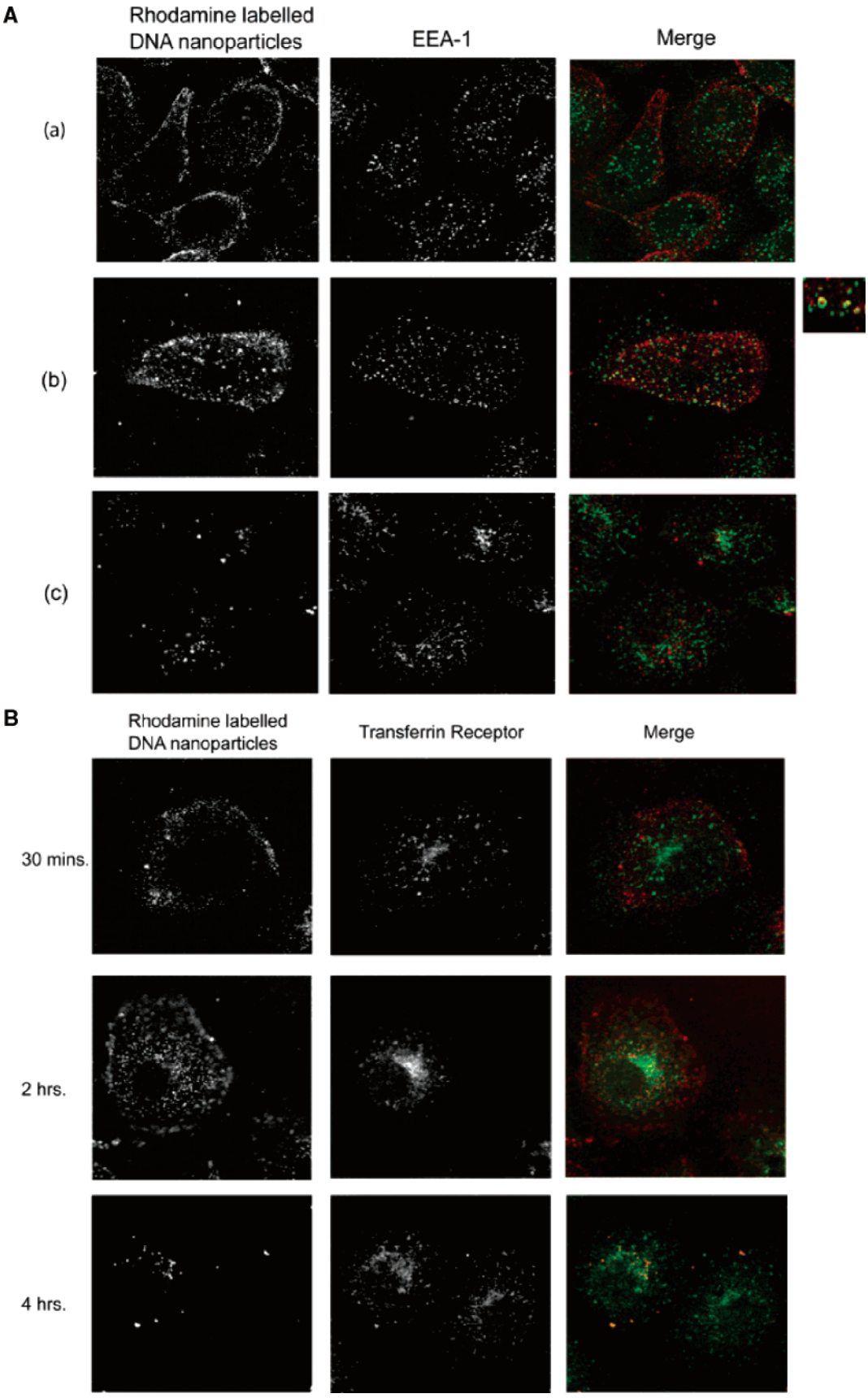

Figure 5. Part 1 of 2.

tosis via the clathrin-dependent pathway. To investigate if, like previous poly-L-lysine vectors, C_1K_{30}−PEG underwent clathrin-mediated endocytosis, the localization of the rhodamine labeled C_1K_{30}−PEG/DNA complexes with respect

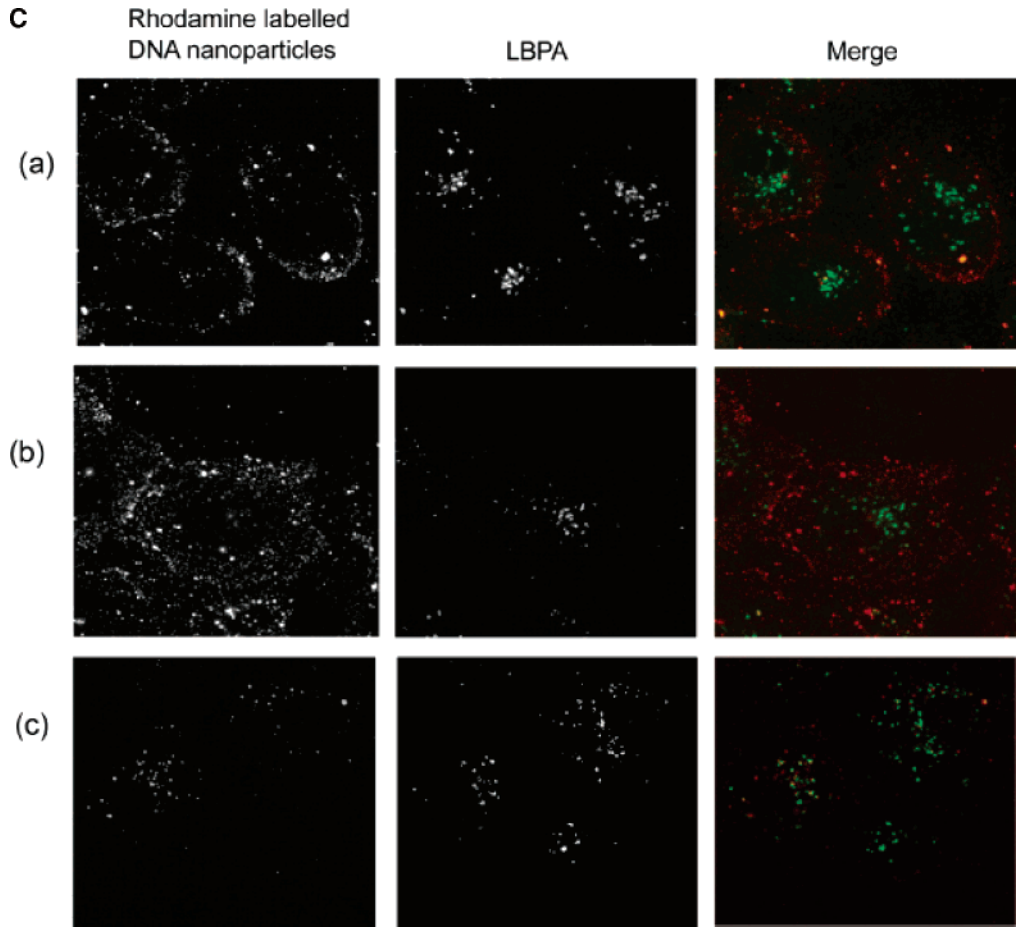

Figure 5. Part 2 of 2. Intracellular trafficking of rhodamine labeled nanoparticles. COS-7 cells were transfected with rhodamine labeled C_1K_{30}−PEG nanoparticles (left panels). At 30 min, 2 h, and 4 h post-transfection, cells were fixed with PFA, permeabilized, and immunostained with antibodies to EEA1 (A), *TfnR* (B), or LBPA (C) as described in the Experimental Section.

to the transferrin receptor (TfnR; a marker of clathrin-coated endosomes) was investigated. The C_1K_{30}−PEG complexes failed to colocalize with TfnR positive vesicles, indicating that the nanoparticles did not enter clathrin-dependent endosomes (Figure 5B). Furthermore, unlike unmodified poly-L-lysine vectors that have been demonstrated to localize to the acidic lysosomes where they undergo degradation,[18] no colocalization of rhodamine labeled complexes and lysobisphosphatidic acid (LBPA) that identifies late endosomes/lysosomes was observed (Figure 5C). Taken together, these data suggest that C_1K_{30}−PEG nanoparticles enter cells via a different pathway than previously described poly-L-lysine vectors.

Nanoparticles Undergo Cellular Entry via Macropinocytosis. To extend these observations and to delineate the entry mechanism of the C_1K_{30}−PEG nanoparticles used in this study, we pretreated COS-7 cells for 1 h with inhibitors of clathrin- and caveolae-mediated uptake (chlorpromazine and filipin III respectively) as well as amiloride, an inhibitor of macropinocytosis.[19,20] Cells were then allowed to internalize rhodamine labeled nanoparticles for 1 h, in the presence of inhibitor, prior to fixation. As demonstrated in Figure 6A, pretreatment of the cells with filipin (2 μg/mL) did not block the entry of the nanoparticles. In chlorpromazine (10 μg/mL) treated cells, a concentration of rhodamine labeling could be seen around the cell periphery (possibly due to chlorpromazine being cytotoxic (Figure 6B)), although intracellular labeling was not reduced. Interestingly, pretreatment of cells with amiloride, a specific inhibitor of the Na^+/H^+ exchange required for macropinocytosis, demonstrated a marked inhibition of nanoparticle entry (Figure 6A). Moreover, amiloride treatment did not demonstrate cytotoxicity (Figure 6B), suggesting that significant nanoparticle entry occurs by lipid-raft mediated macropinocytosis.

Discussion

Conventional treatments for cancer consist of three approaches: surgery, radiotherapy, or chemotherapy. To date, surgical removal of primary tumor tissue remains the principal mode of treatment, but this is frequently combined

(18) Akinc, A.; Langer, R. *Biotechnol. Bioeng.* **2002**, *78* (5), 503−8.
(19) Kee, S. H.; Cho, E. J.; Song, J. W.; Park, K. S.; Baek, L. J.; Song, K. J. *Microbiol. Immunol.* **2004**, *48* (11), 823−9.
(20) Wadia, J. S.; Stan, R. V.; Dowdy, S. F. *Nat. Med.* **2004**, *10* (3), 310−5.

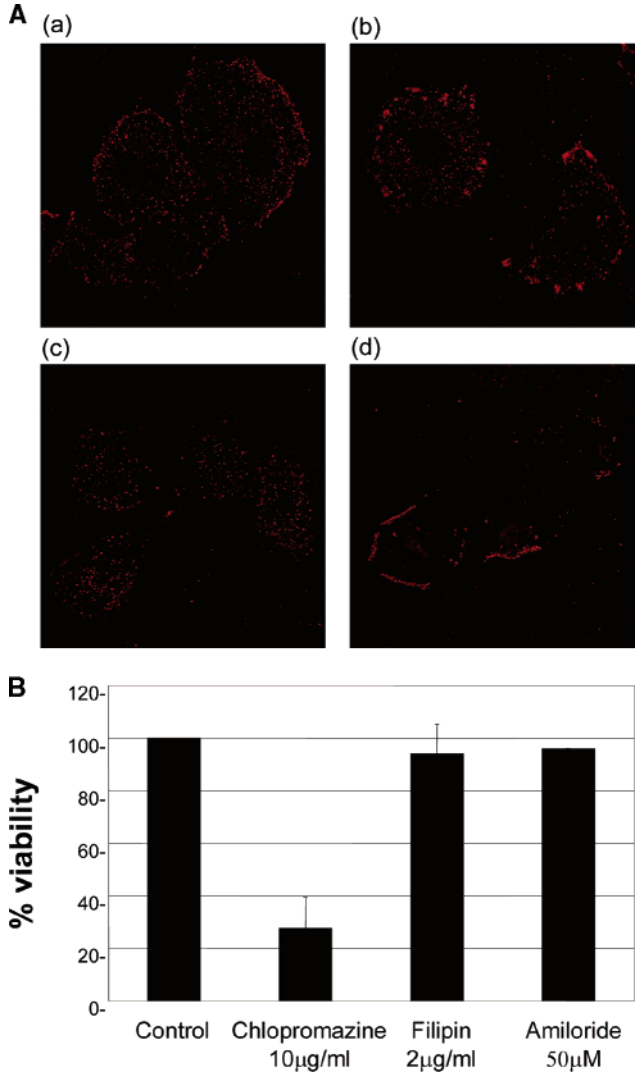

Figure 6. Entry mechanism of C_1K_{30}−PEG nanoparticles. (A) COS-7 cells, grown on coverslips, were either untreated (a) or pretreated in serum free DMEM for 30 min with the following inhibitors; 10 μg/mL chlorpromazine (b), 2 μg/mL filipin III (c), or 50 μM amiloride (d). Cells were then allowed to internalize rhodamine labeled nanoparticles (1 μg of DNA) for 1 h prior to fixation in 3% paraformaldehyde. (B) Cell viability following inhibitor treatment was analyzed by MTT assay. Results are presented as % cell viability relative to control untreated cells.

with chemotherapeutic agents and radioactive isotopes. These classical treatments, however, often face tumors that are drug-resistant, metastatic, or inaccessible. The development of new strategies is a necessary and challenging field of research. Delivery of a therapeutic gene to tumors via nonviral vectors has the potential to be a powerful anticancer tool as gene therapy systems can be designed to target specific tumor types and are less invasive than conventional treatments. The work presented in this paper sought to characterize C_1K_{30}−PEG as a vector for gene delivery to tumors. We demonstrate the amenability of C_1K_{30}−PEG complexes to transfect a growing in vivo tumor mass. We further show, using luciferase gene expression as a measure of transfection efficiency and hence uptake of the various gene delivery vectors, that C_1K_{30}−PEG mediated transfection is significantly higher than unpegylated C_1K_{30}. C_1K_{30}−PEG mediated transfection also compares well to cationic commercially available lipids and polymers and is more efficient than lipofectin and DOTAP. To determine how efficient the C_1K_{30}−PEG nanoparticles are at delivering plasmid DNA into the cell, we investigated the uptake of labeled plasmid following compaction relative to both Lipofectamine 2000 and the unpegylated C_1K_{30} vector. These vectors were chosen for comparative purposes as they demonstrated the most and least efficient transfection relative to the pegylated nanoparticles using luciferase gene expression as a read-out for transfection efficiency. A similar pattern of efficiency to the luciferase expression data was observed. We believe that it is important to note, however, that simply measuring uptake of labeled DNA in the cell may not be a true representation of transfection efficiency as all of these vectors may have different intracellular fates which do not guarantee gene expression. Therefore, coupling an analysis of uptake efficiency with actual gene expression data is much more informative. This of course can only be true once the only variable is the gene delivery vector itself.

The novelty of the C_1K_{30}−PEG nanoparticles is that compared to other commercially available reagents they have a neutral charge. Many modifications have been made to previous nonviral vectors to include specific cell targeting ligands and intracellular targeting moieties such as nuclear localization sequences and endosomal escape agents. We believe that such vector modifications (such as the addition of nuclear localization signals and fusogenic peptides) should be approached with caution as they can have the resultant effect of increasing complex size, which may hinder cellular entry[21] and may also direct vector complexes through otherwise unfavorable pathways. An example of this would be the addition of receptor binding ligands such as epidermal growth factor and transferrin. This could direct complexes to late endosomes/lysosomes or indeed promote recycling back to the cell surface.[22,23] Therefore it is necessary to characterize the uptake mechanism and intracellular trafficking pathway taken by C_1K_{30}−PEG complexes to establish barriers to transfection and to ensure rational vector design.

The inhibitor studies described in this paper suggests that, unlike the aforementioned poly-L-lysine vectors, C_1K_{30}−PEG nanoparticles undergo cellular entry via macropinocytosis. Macropinocytosis is a process that involves the actin-dependent formation of lamellipodia, sheetlike plasma membrane extensions supported by a web of actin filaments. Because macropinosomes are relatively large, they provide an efficient route for nonselective endocytosis of solute macromolecules.[24] Figure 1 shows EM data obtained for the C_1K_{30}−PEG nanoparticles, which are a combination of rod-

(21) Joshee, N.; Bastola, D. R.; Cheng, P. W. *Hum. Gene Ther.* **2002**, *13* (16), 1991−2004.
(22) Sorkin, A. *Biochem. Soc. Trans.* **2001**, *29* (Part 4), 480−4.
(23) Dautry-Varsat, A.; Ciechanover, A.; Lodish, H. F. *Proc. Natl. Acad. Sci. U.S.A.* **1983**, *80* (8), 2258−62.
(24) Swanson, J. A.; Watts, C. *Trends Cell Biol.* **1995**, *5* (11), 424−8.

like or toroid-like structures. When compared with the scale bar, the toroid-like structures display a diameter of ~50 nm. However, the rod-like nanoparticles, while having a smaller diameter of ~20 nm, display lengths of 100−200 nm. Moreover, the EM images fail to show the PEG halo as it is not stained by uranyl acetate and thus not detected by electron microscopy. A 5 kDa PEG should contribute about 28 nm to the diameter of the complexes, although this is not believed to affect the ability of the C_1K_{30}−PEG nanoparticles to enter the nucleus due to the flexible nature of the PEG moieties themselves.[10] Clathrin-coated pits are generally described as having a fairly uniform diameter of 100−200 nm[25] and caveolae that are spherical in shape with a diameter of 50−80 nm.[26] Therefore, as the length of the nanoparticles (100−200 nm) would exceed the diameter of caveolae, their absence from caveolae is not surprising. Clathrin-coated vesicles could accommodate the smaller nanoparticles such as smaller toroid-like structures, although no colocalization was observed between the nanoparticles and the transferrin receptor, a marker of this pathway. The size of the larger toroid-like and rod-like nanoparticles (≥200 nm total diameter) suggests that they could be accommodated in macropinosomes. Why the smaller toroid-like nanoparticles (~90 nm) enter the cell via macropinocytosis rather than via clathrin-dependent endocytosis is unclear, but the less specific nature of the cargo carried in macropinosomes may provide the answer. Uptake of molecules in clathrin-dependent vesicles is cargo dependent and is more or less limited to receptor-bound ligands (receptor-mediated endocytosis). It is unknown and perhaps unlikely that a cell surface receptor exists for C_1K_{30}−PEG and therefore nanoparticle entry into cells via less selective macropinosomes is feasible.

The final destination of the nanoparticles following cellular entry is the perinuclear area of the cell (Figure 4) where most of the rhodamine label appears to concentrate. Similarly to Hewlett and co-workers, who demonstrated that macropinosome content is not delivered to late endosomes,[27] we did not observe colabeling of the C_1K_{30}−PEG nanoparticles with lysosomes, even at 4 h (Figure 5C). It must be noted that while so many results from fixed cells are artifacts of the fixing procedure, any potential artifacts in this study were minimized by the choice of fixative, 3% paraformaldehyde. Furthermore, the intracellular distribution of the nanoparticles is supported by the inhibitor studies further validating our observations.

The ultimate fate of the C_1K_{30}−PEG vector complexes is unclear, but at some stage the C_1K_{30}−PEG vector has to dissociate from the plasmid to allow gene expression. It is likely that the C_1K_{30}−PEG vector may then undergo proteosomal degradation.[28] Whether the vector dissociates from its DNA cargo prior to nuclear entry is unknown, but entry of the intact complexes into the nucleus is possible as an additional advantage of the rod-like structures is their small width of ~20 nm, which may allow them to pass through the 25 nm diameter of the NMP. Therefore, the nanoparticles are capable of transfecting nondividing cells as has been demonstrated by Liu and co-workers.[10] With respect to cancer gene therapy, since not all tumor cells are undergoing cell division simultaneously, any cancer therapeutic strategy targeted toward nondividing cells is significant as it permits more cells receiving plasmid to express the delivered therapeutic gene. From an in vivo gene therapy perspective, the neutral charge on the C_1K_{30}−PEG nanoparticles is an attractive feature. It (a) reduces their aggregation, (b) reduces the possibility of their interaction with negatively charged plasma proteins, an important aspect of cancer gene therapy as tumors tend to be highly vascularized, and (c) increases their solubility. These characteristics make them a more efficient transfection reagent than unmodified polylysine complexes and lends validation to their development for a cancer gene therapy protocol.

Overall, our results delineate a cellular pathway that is likely to influence the efficiency of gene transfer with C_1K_{30}−PEG. The low level of colocalization with early endosomes suggests that addition of a fusogenic peptide or the use of endosomal disrupting agents may not result in increased transfection. However, if targeting to specific tumor types is to be achieved through the addition of receptor binding ligands, the current intracellular pathway of the nanoparticles may be altered. Ligand-dependent, cell surface receptors are frequently internalized by clathrin-mediated endocytosis in which case barriers such as endosomal trafficking to the lysosome may then become significant. Therefore modifications of the C_1K_{30}−PEG vector to improve transfection efficiency need to be more informed with regard to intracellular trafficking pathways as complex trafficking varies greatly with small modifications of the vector. In conclusion, the complete characterization of a nonviral system, from formulation to cellular fate, which maximizes the delivery of DNA to cells, is essential to the successful application of cancer gene therapy regimens.

Acknowledgment. C_1K_{30} peptide was a kind gift from Copernicus Therapeutics. The authors wish to thank Dr. Gerardene Meade of the Royal College of Surgeons of Ireland for help with the confocal microscopy.

MP0600034

(25) Ehrlich, M.; Boll, W.; Van Oijen, A.; Hariharan, R.; Chandran, K.; Nibert, M. L.; Kirchhausen, T. *Cell* **2004**, *118* (5), 591−605.
(26) Pelkmans, L.; Helenius, A. *Traffic* **2002**, *3* (5), 311−20.
(27) Hewlett, L. J.; Prescott, A. R.; Watts, C. *J. Cell Biol.* **1994**, *124* (5), 689−703.
(28) Kim, J.; Chen, C. P.; Rice, K. G. *Gene Ther.* **2005**, *12* (21), 1581−90.